Hindawi Publishing Corporation
Journal of Spectroscopy
Volume 2015, Article ID 350630, 8 pages
http://dx.doi.org/10.1155/2015/350630

*Research Article*

# Spectroscopic Evaluations of Interfacial Oxidative Stability of Phosphonic Nanocoatings on Magnesium

**Anil Mahapatro,[1] Taína D. Matos Negrón,[2] and Alan Nguyen[1]**

[1]*Department of Biomedical Engineering, Wichita State University, Wichita, KS 67260, USA*
[2]*Center for Materials Research (CMR), Norfolk State University, Norfolk, VA 23508, USA*

Correspondence should be addressed to Anil Mahapatro; anil.mahapatro@wichita.edu

Received 8 March 2015; Revised 4 May 2015; Accepted 4 May 2015

Academic Editor: Maria Carmen Yebra-Biurrun



Magnesium (Mg), and its alloys, is being investigated for its potential biomedical applications for its use as a biodegradable metal. However surface modification strategies are needed to modify the surface of the Mg alloy for its applicability in these applications. Self-assembled monolayers (SAMs) have been investigated as a coating strategy on magnesium for biomedical applications. In this report we evaluate the oxidative interfacial stability of phosphonic nanocoatings on magnesium using spectroscopic techniques. Self-assembled mono-/multilayers (SAMs) of octadecylphosphonic acid (ODPA) were formed on the native oxide layer of magnesium alloy using solution deposition technique. The SAMs modified Mg alloy and its oxidative stability were characterized using Fourier transform infrared spectroscopy (FTIR), X-ray photoelectron spectroscopy (XPS), and atomic force microscopy (AFM). FTIR studies indicated mono-/bidentate bonding of the phosphonic SAMs to the Mg alloy surface. XPS confirmed SAM formation showing presence of "P" peaks while consequently showing decrease in peak intensity of Mg peaks. XPS analysis of the phosphonate peaks showed consistent presence of this peak over a period of 21 days. AFM images showed consistent coverage of the Mg alloy over a period of 21 days. The results collectively confirm that the monolayers are stable under the chosen oxidative study.

## 1. Introduction

Magnesium (Mg) based alloys are one of the materials under investigation for their potential applicability as a metallic implant material for applications such as cardiovascular stent, orthopedic scaffold, and fixation devices [1–3]. Mg is a lightweight metal with metallic properties similar to bone and has a natural ionic presence with significant functional roles in the biological system [4, 5]. They could potentially serve as a biocompatible, osteoconductive, degradable metallic scaffold implant for load-bearing orthopedic applications [4–6]. For cardiovascular stent applications, magnesium offers the possibility of better physiological repair and better reconstruction of vascular compliance with minimum inflammatory response [7]. Studies have shown that magnesium ions are able to inhibit platelet activation both by inhibiting certain factors which stimulate the platelets such as Thromboxane A2 and by inhibiting the production of platelet inhibiting factors such as prostacyclin [8, 9]. The in vivo corrosion of magnesium based implant involves the formation of soluble, nontoxic by-products that is harmlessly excreted in the urine [10]. However surface coating strategies are needed to ensure the viability of Mg to be used as a biodegradable metal such as providing a platform for drug and therapeutic delivery for treatment of restenosis and postoperative orthopedic infections, respectively [7, 11].

Self-assembled monolayers (SAMs) are organic assemblies formed by the adsorption of molecular constituents from solution or the gas phase onto the surface of solids [12]. SAMs as a form of nanotechnology are gaining a lot of attention for their potential medical applications due to the ease of modification of surface properties through the selection of the appropriate terminal functional group in the monolayer [13]. In addition, SAMs form structurally well-defined films on solid surface, they form spontaneously and under generally mild conditions, and they can be deposited

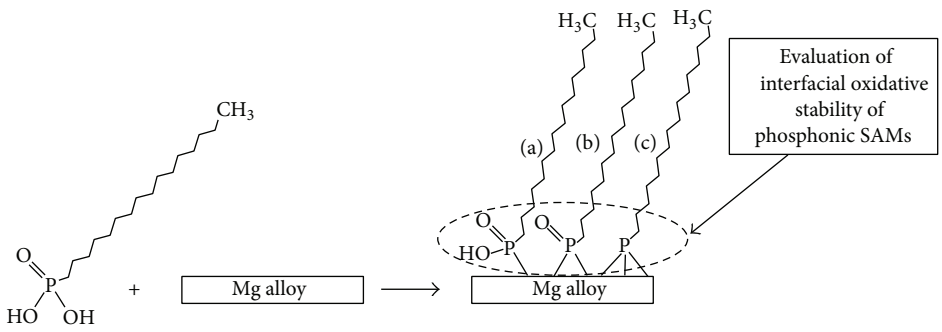


Figure 1: Pictorial representation of phosphonic acid SAMs on Mg alloy.

by a number of easy techniques such as immersing the substrate in solution [14]. The most studied of the SAM systems have been alkanethiol SAMs on gold and other coinage metals [15]. The other well-studied SAM system is SAMs on metal oxide substrates [12, 16, 17]. Phosphonic acids have been gaining a lot of interest as an organic moiety for formation of SAMs due to their ability to bind to a wide range of metal oxide surfaces and form robust SAMs having quality similar to the model system of alkanethiols on Au [14, 18, 19]. Alkyl phosphonic acids are an important class of self-assembling molecules that have been studied on various engineering metal alloys [14, 17, 20, 21]. It has been previously reported that long chain alkylphosphonates form well-ordered and dense monolayers [17, 22]. Octadecylphosphonic acid (ODPA) is a long chain phosphonate and has been widely studied for its bonding with a range of metal oxide systems [14, 20, 23, 24].

Although reports exist on phosphonic SAM formation on biometallic alloys as mentioned above, we could only find few reports investigating the stability of phosphonic SAM systems on biomaterials. Kanta et al. carried out studies to investigate the stability of phosphonic acids formed on titania when immersed in various solvents [25]. They concluded that the phosphonic SAMs on titania were stable after immersion for 18 hr in different organic solvents. Mani et al. reported the stability of phosphonic acid on titanium and compared it with the stability of alkanethiol on Au [26]. They concluded that phosphonic SAMs of hydroxyl terminated (11-hydroxyundecyl) phosphonic acid were stable on the surface of titanium for up to a period of 14 days of ambient air exposure without any significant desorption. We could not find any reports of oxidative stability of phosphonic SAMs on Mg alloy. In this paper we present results analyzing the oxidative interfacial stability of phosphonic self-assembled monolayers on Mg alloy. Oxidative stability would be a prerequisite prior to physiological and biological stability. Methyl terminated ODPA SAMs having uniform surface coverage on Mg alloy were formed using solution deposition technique. Ambient laboratory conditions were used as oxidative conditions for determining the stability of the SAMs. The resulting monolayers were characterized using XPS, FTIR, and AFM. The oxidative stability of the SAMs was evaluated over a period of 21 days.

## 2. Experimental Section

Octadecylphosphonic acid ($C_{18}H_{39}PO_3$, ODPA, 98% purity) was purchased from Alfa Aesar and used as received without further purification. Ethanol (200 proof), acetone (99.5% purity), and dimethyl sulfoxide (DMSO, 98.5 purity) were also used as received without further purification from Sigma-Aldrich. Magnesium alloys (Mg 96%/Al 3%/Zn 1%; 0.25 mm and 1.0 mm thickness) were purchased from Goodfellow Inc., Oakdale, PA. Magnesium alloy sheets were cut into squares (10 mm × 10 mm × 0.25 mm) and were used as substrate for SAM formation. The substrates were cleaned by ultrasonication in acetone and ethanol for 10 minutes each. The substrates were then rinsed with d-$H_2O$ and dimethyl sulfoxide (DMSO) and dried with air and subsequently used for SAM formation. Cleaned (described above) Mg substrates were immersed in 30 mL of 2 mmol 18-octadecylphosphonic acid ($C_{18}H_{39}PO_3$) solution in DMSO. The octadecylphosphonic acid solution was maintained at 35°C for 48 hours. After the 48-hour reaction time was complete, samples were rinsed using DMSO and ultrasonicated for three minutes in deionized $H_2O$ to remove any excess surfactant. The samples were air-dried immediately and characterized. ODPA-coated SAMs (Figure 1) were exposed to light under ambient laboratory conditions after SAM formation for 1, 3, 7, 14, and 21 days. After oxidative exposure, samples were ultrasonicated for 3 minutes, rinsed in deionized water, air-dried, and transferred to polyethylene wafer containers, which were kept in a desiccator purged with argon until further characterization.

### 2.1. Characterization of the Monolayers

*2.1.1. Fourier Transform Infrared Spectroscopy (FTIR).* SAM modified Mg samples were characterized with Fourier transform infrared spectroscopy (FTIR). The FTIR spectra from the substrates were acquired using attenuated total reflectance (ATR) FTIR (Bruker IFS66 FTIR/Raman FRA 106/S Unit). The spectra were recorded under dry air purged system conditions to eliminate the background signal due to $CO_2$ and $H_2O$ absorption bands. The unmodified Mg substrates were used as background spectra for analysis purposes. All spectra were obtained with 2 $cm^{-1}$ resolution after 1024 scans.

Table 1: XPS determined % atomic concentrations of bulk Mg alloy and SAMs on Mg alloy.

| Sample | Mg 1s | C 1s | O 1s | P 2p |
|---|---|---|---|---|
| Mg (control) | 11.14 ± 2.2 | 27.5 ± 3.1 | 60.7 ± 3.7 | — |
| OPDA | 2.67 ± 0.2 | 59.7 ± 1.9 | 35.3 ± 1.2 | 1.73 ± 0.1 |

*2.1.2. X-Ray Photoelectron Spectroscopy (XPS).* XPS was used to evaluate the surface composition and chemistry of the SAMs formed on Mg alloy. XPS data was taken on a Kratos Axis Ultra DLD spectrometer equipped with a monochromatic Al K$\alpha$ X-ray source (15 kV, 225 W, and base pressure 5–$10^{-10}$ torr). Survey spectra were obtained at a pass energy of 80 eV, while high resolution scans were obtained at a pass energy of 20 eV from a 0.37 × 1.0 $mm^2$ area of the sample. The binding energies were corrected by referencing the C 1s binding energy to 285 eV.

*2.1.3. Atomic Force Microscope (AFM).* AFM was used to evaluate the surface topography before and after the formation of the SAM layers. AFM imaging of the samples was performed in tapping mode at ambient conditions using silicon tips. Scan rates of 0.5 Hz were used for tapping mode. The surface roughness analysis on the two-dimensional topography was based on a calculation of the standard deviation of all height values within the given imaged area (root-mean-square roughness (rms)).

## 3. Results and Discussion

Films of phosphonic acids were formed on Mg alloy samples by solution immersion technique. XPS was used to verify SAM formation on Mg alloy and to determine the surface compositions of Mg alloy before and after ODPA deposition. Typical XPS survey spectra of Mg alloy (control) and on modified surfaces are shown in Figure 2. The blank Mg alloy sample showed presence of Mg 1s, Mg *2s*, O 1s, C 1s, and other constituent alloy elements peaks (Figure 2). The surface elemental compositions of plain Mg sample and ODPA modified Mg sample are summarized in Table 1. The plain Mg alloy had a surface oxygen concentration of 60.7% wt, Mg concentration of 11.14% wt, and carbon concentration of 27.5% wt. The deviation of our surface oxide composition (Table 1) from the bulk metal composition (Table 1) is in agreement with published reports on XPS analysis of metallic surface oxide compositions [30, 31]. The excessive carbon can be explained as a result of formation of a carbonaceous contamination overlayer. Carbon contaminant is unavoidable aspect of the deposition procedure and it is detected in the surface sensitive XPS signal, as any sample exposed to atmosphere tends to pick up hydrophobic and hydrophilic hydrocarbon contaminants. This excess carbon atmospheric contamination has been similarly reported in previous literatures [14, 32, 33]. After ODPA adsorption, a significant increase in carbon concentration is observed (Table 1), concurrent with the appearance of P *2s* and P *2p* signals at 192.2 eV and 130.5 eV (see Figure 2 and Table 1).

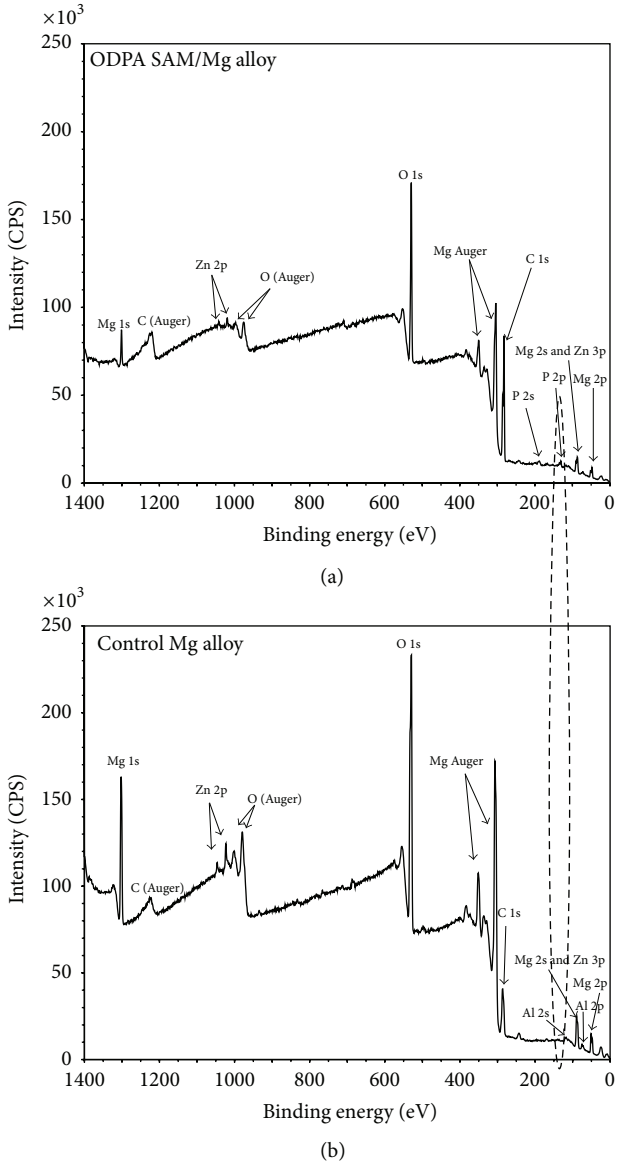


Figure 2: XPS survey spectra of control magnesium alloy (b) and of ODPA SAM on Mg alloy (a).

These values are in good agreement with earlier reported values for ODPA SAMs on steel [20] and Co-Cr alloy [14]. The measured intensities for Mg and other metals decrease after ODPA adsorption (Figure 2) with the appearance of the "P" peak (Figures 2 and 3). XPS results thus indicate presence of "P" on the metal confirming the formation of phosphonic SAMs on Mg alloy. The ratio of the surface carbon "C" concentration to the phosphorus "P" concentration was found to be 30 (±1.32) and is nearly twice the expected value of 18 for the C to P ratio of the ODPA ($C_{18}H_{39}PO_3$) molecule. This observation suggests the continued presence of atmospheric C contaminants on top of the ODPA layers on the surface as observed with the control Mg alloy sample. A comparison of the O 1s spectrum of the Mg alloy and ODPA-coated Mg alloy (Figure 4) gives an indication of the change in oxygen "O" bonding coordination on the surface before

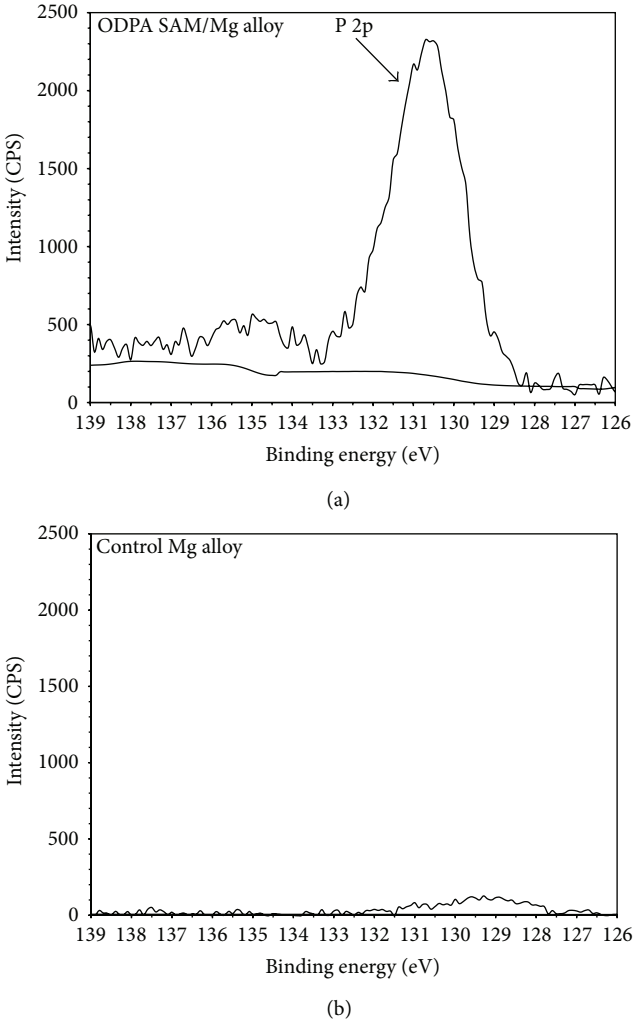


Figure 3: XPS P 2p region of control Mg alloy (b) and ODPA modified SAM Mg alloy (a).

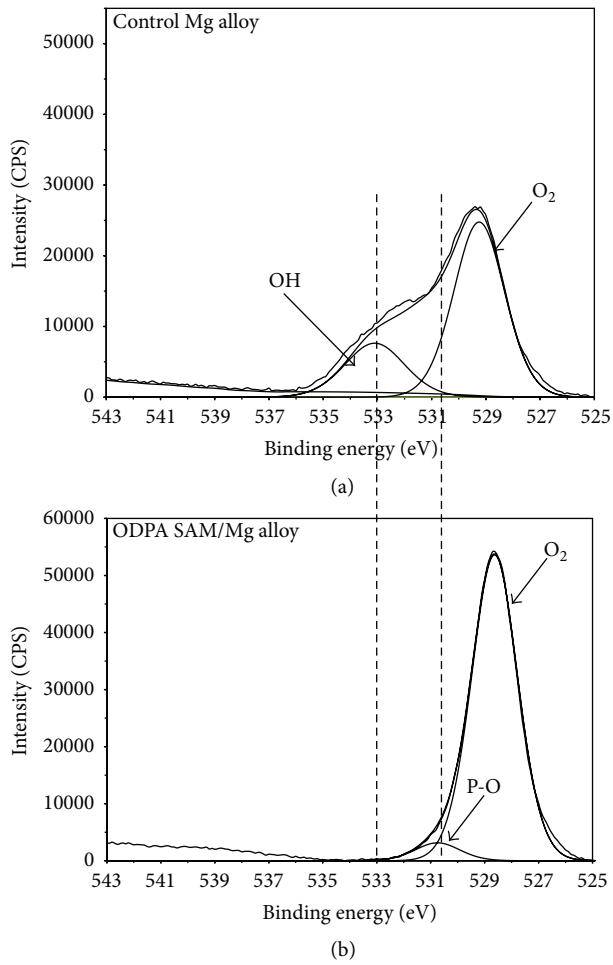


Figure 4: XPS O 1s spectra of bare Mg alloy (control, (a)) and ODPA modified SAM Mg alloy (b).

Table 2: FTIR assignments and positions of the vibrational bands of 18-octadecylphosphonic acid self-assembled layers [17, 20, 27–29].

| Assignments | Experimental wavenumber ($cm^{-1}$) |
|---|---|
| $\nu$ op($CH_3$) | 2960 |
| $\nu$ asym($CH_2$) | 2921.7 |
| $\nu$ sym($CH_2$) | 2850 |
| $\nu$ (P–O) | 1095.4 |
| $\nu$ (P=O) | 1261.2 |
| $\nu$ (P–OH) | 873.6 |

and after deposition. From the O 1s deconvolution analysis of untreated Mg substrate the O 1s peak at 528.4 eV and 530.5 eV has been attributed to surface oxides and surface hydroxides, respectively [34]. Deconvolution of O 1s spectrum of OPDA-coated Mg substrate showed presence of P–O (O 1s = 531 eV), which appears after the deposition of ODPA.

ATR-FTIR was used to further characterize SAM formation and order. Table 2 shows the assignments of our experimental FTIR vibrational spectra bands of 18-octadecylphosphonic acid (ODPA) layers on Mg alloy. For our samples the peak frequencies of $\nu CH_{2\ sym}$ and $\nu CH_{2\ asym}$ for the ODPA layers prepared on Mg alloy were found to be at 2850 $cm^{-1}$ and 2921.7 $cm^{-1}$, respectively (Table 2). These two frequency positions are for the symmetric and asymmetric methylene stretching and indicate that the methylene chains in ODPA layers on Mg alloy are ordered and predominantly have "all-trans" interactions. The peak at 2960 $cm^{-1}$ is assigned to the out-of-plane asymmetric methyl stretching mode $\nu CH_{3op}$ [17, 27]. These results are in agreement with those obtained for ODPA on nitinol, GaN, and 316L SS [17, 28, 35]. Also since our spectra were obtained after sonicating the substrate with DMSO and $dH_2O$ to remove weakly bound material, we can conclude that the SAM film is strongly bound to the surface of the substrate. Table 2 also shows the shifts of the ATR-FTIR spectra of ODPA SAMs in the P–O region. The nature of the interaction between the SAM molecules and surface can be determined from the shifts and broadening of $\nu_{P=O}$, $\nu_{P-O}$, and $\nu_{P-OH}$ peaks. The P–O region of the ODPA SAM sample (Table 2) contained broad P–O peak frequencies such as $\nu_{P=O}$

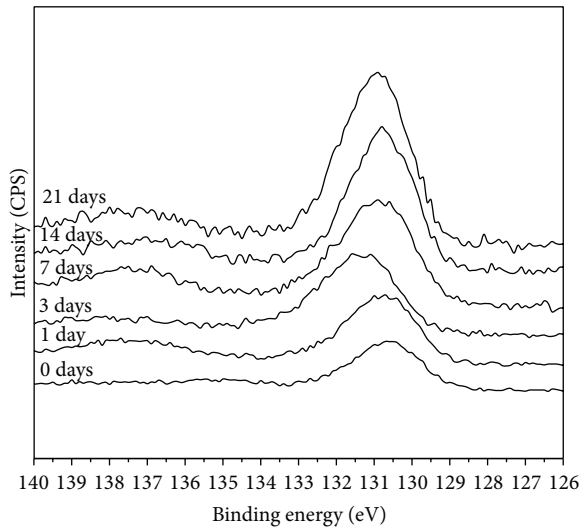


Figure 5: XPS P 2p spectra evaluating oxidative stability for ODPA SAMs (1–21 days) with respect to freshly prepared SAMs (0 days).

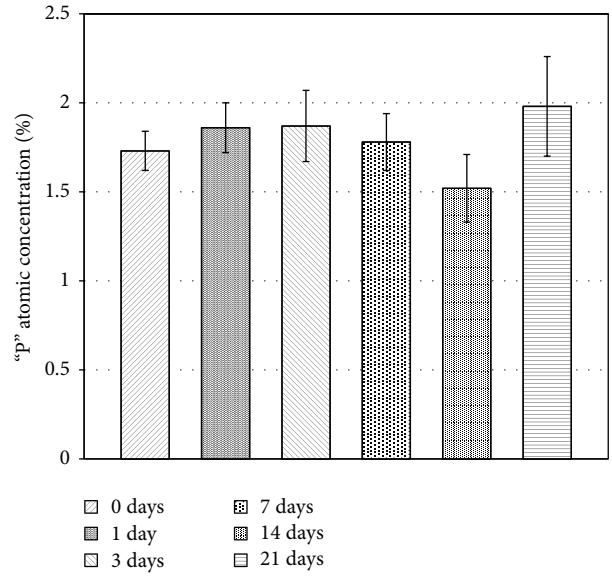


Figure 6: XPS % "P" concentration evaluating oxidative stability for ODPA SAMs (1–21 days) with respect to freshly prepared SAMs (0 days).

at 1261.2 $cm^{-1}$, $\nu_{P-O}$ at 1095.4 $cm^{-1}$, and $\nu_{P-OH}$ at 873.6 $cm^{-1}$. These observed frequencies for P=O, P–O, and P–OH are in good agreement with the FTIR stretching of these bonds in other phosphonate systems such as phosphonate SAMs on nitinol [35]. The phosphonic SAMs can bind to the Mg alloy in three different ways: monodentate, bidentate, and tridentate bonding configurations (Figure 1). Since we see the presence of all possible PO stretching scenarios (P=O, P–O, and P–OH) we can eliminate the "tridentate" bonding possibility. Thus the bonding of the SAMs to Mg alloy is proposed to be entirely monodentate or a combination of mono- and bidentate bonding. These bonding scenarios are in agreement with possible bonding of phosphonic SAMs on other metal oxide systems [14, 17, 20, 21].

To evaluate the oxidative stability of phosphonic SAMs on Mg alloy, detailed high energy elemental XPS scans of the "P" region were taken and the % element composition of "P" was calculated based on the P 2p peaks which represent the metal phosphonate peak. Figure 5 shows the detailed high energy XPS scan for the P 2p region over the period of the oxidative stability studies. The 0-day SAMs sample represents the freshly formed ODPA SAMs on Mg alloy surface. The spectra for control Mg (Figure 3) showed no P 2p peaks present. The variation of the % "P" atomic concentration gives an indication of the variation of SAM presence on the surface which is correlated to the oxidative stability of the SAMs. Figure 5 shows the strong presence of the P 2p peak over the duration of oxidative stability study. The P 2p peak which is centered around 130.5 eV is very consistent for 1, 3, 7, 14, and 21 days of oxidative exposure. Figure 6 shows the % "P" atomic concentration as determined by XPS over period of 21 days after oxidative exposure. The % P atomic concentration was found to be consistent over the duration of study. This indicated that the SAMs were strongly bound to the metal alloy even after 21 days. This result is in agreement with other phosphonic SAM stability studies on stronger metal oxide systems such as Co-Cr alloy [36].

Atomic force microscopy was used to characterize the topography of the Mg surface before and after SAM formation and during the course of oxidative stability studies. The AFM images were carried out using tapping mode in air. The root-mean-square (rms) roughness parameter is a measure of the deviations in the surface from the mean plane within the sampling area. The rms roughness parameter gives us an insight into variations in surface height and its uniformity. The rms roughness of the control and modified substrates were compared. SAMs modified surfaces with similar rms roughness to the control surface are considered to be coated with monolayer films that follow the contour of the surface, while modified surfaces that have large deviance of rms roughness from the control are considered to be coated with multilayers [14, 19, 33, 37]. The samples were scanned over 5 $\mu m^2$ region for Mg alloy (control) and for ODPA sample. The plain Mg alloy control sample had an rms roughness of 11.6 nm ± 0.25 and revealed a nonuniform contour with well-defined islands (see Figure 7). Deposition of the ODPA SAMs (Figure 6) above the Mg alloy resulted in a decrease of the rms roughness value from 11.6 ± 0.25 nm to 2.3 ± 0.27 nm (Table 3). This lowering of the rms roughness value suggests the possibility of formation of mono-/multilayers of ODPA on Mg alloy. Figure 6 shows areas of formation of ODPA islands and aggregates on the surface of the substrates. Island formation as observed on ODPA SAM deposited Mg surfaces is in agreement with previous work investigating SAM formation on bulk sample surfaces versus sputter coated sample surfaces which showed that the bulk sample surfaces showed larger island formation due to inherent roughness of the base surface [14, 33]. Figure 7 also shows the representative AFM 3D topographical images of ODPA SAMs on Mg alloy after

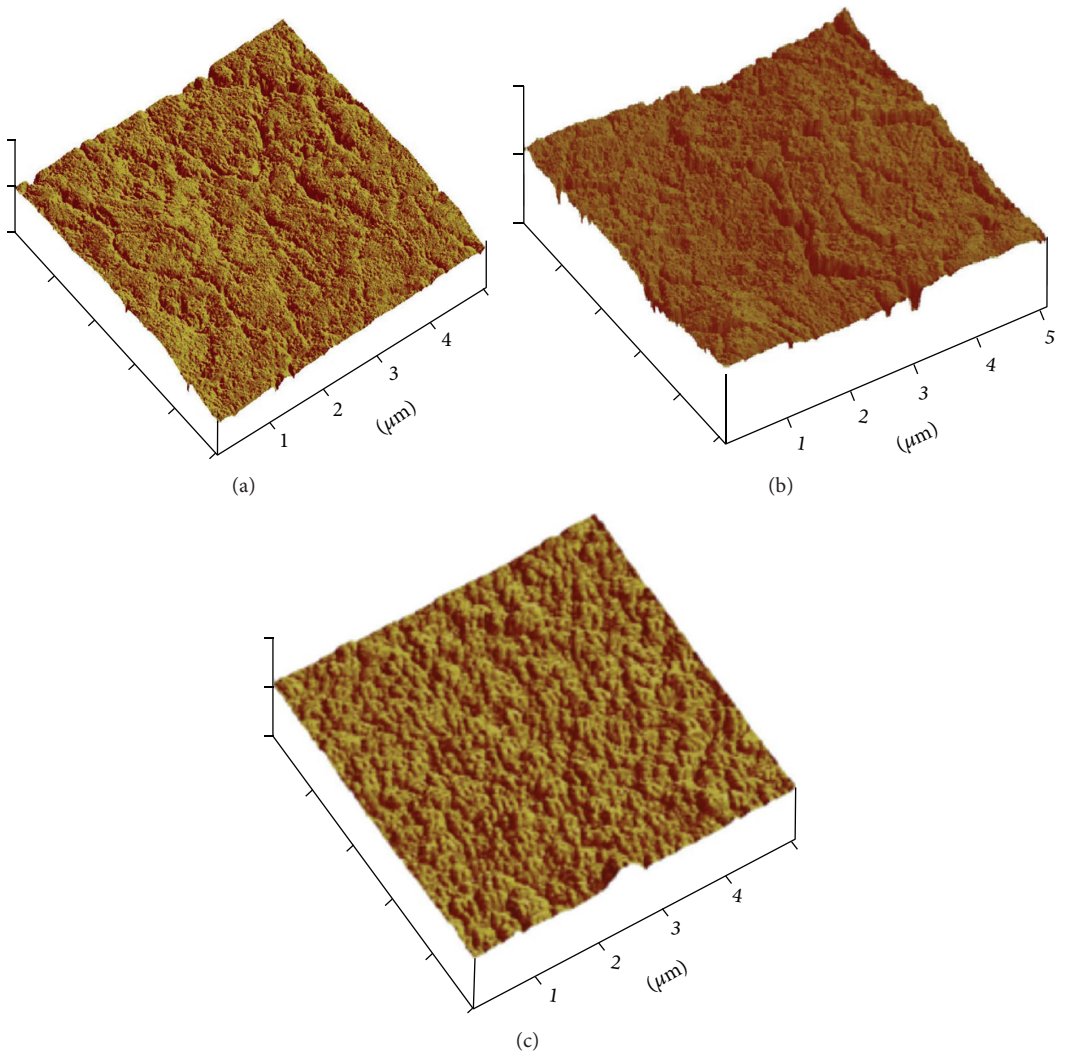


Figure 7: AFM images of clean Mg alloy (a), fresh Mg SAM (b), and 21-day Mg SAM (c).

oxidative exposure of 21 days. After 21 days we still observe a continuation of the regular pattern of islands of SAMs which are uniformly covered over the surface. The rms roughness values were obtained for control, freshly prepared SAMs, and SAM samples exposed for a period of 21 days (Table 3). The rms values of samples over the period of oxidative stability study remained approximately the same (Table 3). Previously reported literature suggests that there is a large variation of rms roughness values for SAM coating by solution deposition on account of exposure to various environmental conditions including ambient air [38]. It is also believed that the sample preparation and characterization processes also play a role in the large variation of the rms roughness values. Other factors possibly contributing to this variation include substrate morphology, substrate chemical composition, surface oxide chemistry, surface pretreatment procedures, and the nature of SAM being deposited on the substrate [33]. The rms value of the plain Mg sample (11.6 ± 0.25 nm) indicates that the Mg alloy itself is very rough. This relative roughness of the Mg based alloy affects the final monolayer formation kinetics and plays a major role in determining the structure and uniformity of the SAM formation. Thus based on the topographical images and the roughness analyses of our samples, we conclude that the ODPA SAMs do not show significant deviation within the samples tested.

Table 3: Surface rms values variation over time.

| Sample | rms value (nm) |
|---|---|
| Plain Mg (control) | 11.6 ± 0.25 |
| 0-day Mg SAM | 2.30 ± 0.27 |
| 1-day Mg SAM | 2.63 ± 0.29 |
| 3-day Mg SAM | 2.82 ± 0.09 |
| 7-day Mg SAM | 2.68 ± 0.33 |
| 14-day Mg SAM | 2.81 ± 0.23 |
| 21-day Mg SAM | 2.99 ± 0.34 |

## 4. Conclusions

In summary, SAMs of octadecylphosphonic acid were successfully formed on the oxide surface of Mg alloy using solution immersion method. FTIR, XPS, and AFM measurements collectively confirm SAM formation on Mg alloy. FTIR studies indicated mono-/bidentate bonding of the phosphonic SAMs to the Mg alloy surface. XPS confirmed SAM formation showing presence of P peaks while consequently showing decrease in peak intensity of Mg peaks. XPS analysis of the phosphonate peaks showed consistent presence of this peak over a period of 21 days. AFM topographical images showed consistent coverage of the Mg alloy over a period of 21 days. Thus the results collectively confirm that the monolayers are stable under the chosen oxidative study.

## Conflict of Interests

The authors declare that there is no conflict of interests regarding the publication of this paper.

## Acknowledgments

The authors would like to acknowledge Wichita State University and the Center of Biotechnology and Biomedical Sciences (CBBS) at Norfolk State University for partial support of the work. They would like to acknowledge the surface characterization lab of the College of William and Mary at Applied Research Center, Jefferson Labs, Newport News, for their assistance with AFM experiments.

## References

[1] H. Waizy, J.-M. Seitz, J. Reifenrath et al., "Biodegradable magnesium implants for orthopedic applications," *Journal of Materials Science*, vol. 48, no. 1, pp. 39–50, 2013.

[2] H. Hermawan, D. Dubé, and D. Mantovani, "Developments in metallic biodegradable stents," *Acta Biomaterialia*, vol. 6, no. 5, pp. 1693–1697, 2010.

[3] A. Mahapatro, "Metals for biomedical applications and devices," *Journal of Biomaterials and Tissue Engineering*, vol. 2, no. 4, pp. 259–268, 2012.

[4] J. Vormann, "Magnesium: nutrition and metabolism," *Molecular Aspects of Medicine*, vol. 24, no. 1–3, pp. 27–37, 2003.

[5] T. Okuma, "Magnesium and bone strength," *Nutrition*, vol. 17, no. 7-8, pp. 679–680, 2001.

[6] F. Witte, N. Hort, C. Vogt et al., "Degradable biomaterials based on magnesium corrosion," *Current Opinion in Solid State and Materials Science*, vol. 12, no. 5-6, pp. 63–72, 2008.

[7] M. Moravej and D. Mantovani, "Biodegradable metals for cardiovascular stent application: interests and new opportunities," *International Journal of Molecular Sciences*, vol. 12, no. 7, pp. 4250–4270, 2011.

[8] P. Delva, "Magnesium and coronary heart disease," *Molecular Aspects of Medicine*, vol. 24, no. 1–3, pp. 63–78, 2003.

[9] P. Lu, H. Fan, Y. Liu, L. Cao, X. Wu, and X. Xu, "Controllable biodegradability, drug release behavior and hemocompatibility of PTX-eluting magnesium stents," *Colloids and Surfaces B: Biointerfaces*, vol. 83, no. 1, pp. 23–28, 2011.

[10] M. P. Staiger, A. M. Pietak, J. Huadmai, and G. Dias, "Magnesium and its alloys as orthopedic biomaterials: a review," *Biomaterials*, vol. 27, no. 9, pp. 1728–1734, 2006.

[11] D. Y. Kwon, J. I. Kim, D. Y. Kim et al., "Biodegradable stent," *Journal of Biomedical Science and Engineering*, vol. 5, pp. 212–220, 2012.

[12] R. Bhure and A. Mahapatro, "Silicon based nanocoatings on metal alloys and their role in surface engineering," *Silicon*, vol. 2, no. 3, pp. 117–151, 2010.

[13] D. G. Castner and B. D. Ratner, "Biomedical surface science: foundations to frontiers," *Surface Science*, vol. 500, no. 1–3, pp. 28–60, 2002.

[14] R. Bhure, T. M. Abdel-Fattah, C. Bonner, J. C. Hall, and A. Mahapatro, "Formation of nanosized phosphonic acid self assembled monolayers on cobalt-chromium alloy for potential biomedical applications," *Journal of Biomedical Nanotechnology*, vol. 6, no. 2, pp. 117–128, 2010.

[15] J. C. Love, L. A. Estroff, J. K. Kriebel, R. G. Nuzzo, and G. M. Whitesides, "Self-assembled monolayers of thiolates on metals as a form of nanotechnology," *Chemical Reviews*, vol. 105, no. 4, pp. 1103–1169, 2005.

[16] S. Onclin, B. J. Ravoo, and D. N. Reinhoudt, "Engineering silicon oxide surfaces using self-assembled monolayers," *Angewandte Chemie—International Edition*, vol. 44, no. 39, pp. 6282–6304, 2005.

[17] W. Gao, L. Dickinson, C. Grozinger, F. G. Morin, and L. Reven, "Self-assembled monolayers of alkylphosphonic acids on metal oxides," *Langmuir*, vol. 12, no. 26, pp. 6429–6435, 1996.

[18] D. M. Spori, N. V. Venkataraman, S. G. P. Tosatti, F. Durmaz, N. D. Spencer, and S. Zürcher, "Influence of alkyl chain length on phosphate self-assembled monolayers," *Langmuir*, vol. 23, no. 15, pp. 8053–8060, 2007.

[19] R. Bhure, T. M. Abdel-Fattah, C. Bonner, F. Hall, and A. Mahapatro, "Stability of phosphonic self assembled monolayers (SAMs) on cobalt chromium (Co–Cr) alloy under oxidative conditions," *Applied Surface Science*, vol. 257, no. 13, pp. 5605–5612, 2011.

[20] A. Raman, M. Dubey, I. Gouzman, and E. S. Gawalt, "Formation of self-assembled monolayers of alkylphosphonic acid on the native oxide surface of SS316L," *Langmuir*, vol. 22, no. 15, pp. 6469–6472, 2006.

[21] N. Adden, L. J. Gamble, D. G. Castner, A. Hoffmann, G. Gross, and H. Menzel, "Phosphonic acid monolayers for binding of bioactive molecules to titanium surfaces," *Langmuir*, vol. 22, no. 19, pp. 8197–8204, 2006.

[22] R. Helmy and A. Y. Fadeev, "Self-assembled monolayers supported on $TiO_2$: comparison of $C_{18}H_{37}SiX_3$ (X = H, Cl, $OCH_3$), $C_{18}H_{37}Si(CH_3)_2Cl$, and $C_{18}H_{37}PO(OH)_2$," *Langmuir*, vol. 18, no. 23, pp. 8924–8928, 2002.

[23] E. S. Gawalt, M. J. Avaltroni, N. Koch, and J. Schwartz, "Self-assembly and bonding of alkanephosphonic acids on the native oxide surface of titanium," *Langmuir*, vol. 17, no. 19, pp. 5736–5738, 2001.

[24] A. Raman and E. S. Gawalt, "Self-assembled monolayers of alkanoic acids on the native oxide surface of SS316L by solution deposition," *Langmuir*, vol. 23, no. 5, pp. 2284–2288, 2007.

[25] A. Kanta, R. Sedev, and J. Ralston, "The formation and stability of self-assembled monolayers of octadecylphosphonic acid on titania," *Colloids and Surfaces A: Physicochemical and Engineering Aspects*, vol. 291, no. 1–3, pp. 51–58, 2006.

[26] G. Mani, D. M. Johnson, D. Marton et al., "Stability of self-assembled monolayers on titanium and gold," *Langmuir*, vol. 24, no. 13, pp. 6774–6784, 2008.

[27] M. D. Porter, T. B. Bright, D. L. Allara, and C. E. D. Chidsey, "Spontaneously organized molecular assemblies. 4. Structural characterization of n-alkyl thiol monolayers on gold by optical ellipsometry, infrared spectroscopy, and electrochemistry," *Journal of the American Chemical Society*, vol. 109, no. 12, pp. 3559–3568, 1987.

[28] R. Quiñones and E. S. Gawalt, "Study of the formation of self-assembled monolayers on nitinol," *Langmuir*, vol. 23, no. 20, pp. 10123–10130, 2007.

[29] P. Fiurasek and L. Reven, "Phosphonic and sulfonic acid-functionalized gold nanoparticles: a solid-state NMR study," *Langmuir*, vol. 23, no. 5, pp. 2857–2866, 2007.

[30] T. Hanawa, S. Hiromoto, and K. Asami, "Characterization of the surface oxide film of a Co-Cr-Mo alloy after being located in quasi-biological environments using XPS," *Applied Surface Science*, vol. 183, no. 1-2, pp. 68–75, 2001.

[31] R. Bhure, A. Mahapatro, C. Bonner, and T. M. Abdel-Fattah, "In vitro stability study of organophosphonic self assembled monolayers (SAMs) on cobalt chromium (Co–Cr) alloy," *Materials Science and Engineering C*, vol. 33, no. 4, pp. 2050–2058, 2013.

[32] A. Mahapatro, D. M. Johnson, D. N. Patel, M. D. Feldman, A. A. Ayon, and C. M. Agrawal, "The use of alkanethiol self-assembled monolayers on 316L stainless steel for coronary artery stent nanomedicine applications: an oxidative and in vitro stability study," *Nanomedicine: Nanotechnology, Biology, and Medicine*, vol. 2, no. 3, pp. 182–190, 2006.

[33] G. Mani, M. D. Feldman, S. Oh, and C. M. Agrawal, "Surface modification of cobalt-chromium-tungsten-nickel alloy using octadecyltrichlorosilanes," *Applied Surface Science*, vol. 255, no. 11, pp. 5961–5970, 2009.

[34] I. Gouzman, M. Dubey, M. D. Carolus, J. Schwartz, and S. L. Bernasek, "Monolayer vs. multilayer self-assembled alkylphosphonate films: X-ray photoelectron spectroscopy studies," *Surface Science*, vol. 600, no. 4, pp. 773–781, 2006.

[35] R. Quiñones, A. Raman, and E. S. Gawalt, "Functionalization of nickel oxide using alkylphosphonic acid self-assembled monolayers," *Thin Solid Films*, vol. 516, no. 23, pp. 8774–8781, 2008.

[36] R. Bhure, T. M. Abdel-Fattah, C. Bonner, F. Hall, and A. Mahapatro, "Stability of phosphonic self assembled monolayers (SAMs) on cobalt chromium (Co–Cr) alloy under oxidative conditions," *Applied Surface Science*, vol. 257, no. 13, pp. 5605–5612, 2011.

[37] R. Quiñones, A. Raman, and E. S. Gawalt, "An approach to differentiating between multi- and monolayers using MALDI-TOF MS," *Surface and Interface Analysis*, vol. 39, no. 7, pp. 593–600, 2007.

[38] D. F. S. Petri, G. Wenz, P. Schunk, and T. Schimmel, "An improved method for the assembly of amino-terminated monolayers on $SiO_2$ and the vapor deposition of gold layers," *Langmuir*, vol. 15, no. 13, pp. 4520–4523, 1999.